JPRAS Open 14 (2017) 39–48

Contents lists available at ScienceDirect

JPRAS Open

journal homepage: http://www.journals.elsevier.com/jpras-open

Original Article

Accuracy of generic mesh conformation: The future of facial morphological analysis

A. Almukhtar [a], B. Khambay [b], X. Ju [c, d], J. McDonald [d], A. Ayoub [e, *]

[a] Scottish Craniofacial Research Group, Glasgow Dental School, University of Glasgow, Glasgow, UK
[b] Institute of Clinical Sciences, College of Medical and Dental Sciences, The School of Dentistry, University of Birmingham, Birmingham, UK
[c] Medical Device Unit, Department of Clinical Physics and Bioengineering, NHS Greater Glasgow and Clyde, Glasgow, UK
[d] Glasgow Dental School, University of Glasgow, Glasgow, UK
[e] MVLS College, Medical School, University of Glasgow, Glasgow, UK

ARTICLE INFO

Article history:
Received 17 November 2016
Accepted 5 August 2017
Available online 30 August 2017

Keywords:
3D
Face
Deformities
Analysis
Mesh

ABSTRACT

Three-dimensional (3D) analysis of the face is required for the assessment of changes following surgery, to monitor the progress of pathological conditions and for the evaluation of facial growth. Sophisticated methods have been applied for the evaluation of facial morphology, the most common being dense surface correspondence. The method depends on the application of a mathematical facial mask known as the generic facial mesh for the evaluation of the characteristics of facial morphology. This study evaluated the accuracy of the conformation of generic mesh to the underlying facial morphology. The study was conducted on 10 non-patient volunteers. Thirty-four 2-mm-diameter self-adhesive, non-reflective markers were placed on each face. These were readily identifiable on the captured 3D facial image, which was captured by Di3D stereophotogrammetry. The markers helped in minimising digitisation errors during the conformation process. For each case, the face was captured six times: at rest and at the maximum movements of four facial expressions. The 3D facial image of each facial expression was analysed. Euclidean distances between the 19 corresponding landmarks on the conformed mesh and on the original 3D facial model provided a measure of the accuracy of the conformation process. For all facial expressions and all corresponding landmarks, these distances were between 0.7 and 1.7 mm. The absolute mean distances ranged from 0.73 to 1.74 mm. The mean absolute error of the conformation process was 1.13 ± 0.26 mm. The conformation of the generic facial mesh

* Corresponding author. Glasgow University, 378 Sauchiehall Street, G2 3JZ, UK.
E-mail address: ashraf.ayoub@glasgow.ac.uk (A. Ayoub).

http://dx.doi.org/10.1016/j.jpra.2017.08.003

is accurate enough for clinical trial proved to be accurate enough for the analysis of the captured 3D facial images.

Introduction

At present, the analysis of three-dimensional (3D) facial images has generally been limited to linear and angular measurements between anatomical landmarks. The operator usually identifies and digitises a set of landmarks that result in a 3D landmark configuration, which is then used for analysis. The limited number of accurately identifiable landmarks does not allow a comprehensive analysis of the facial morphology.

To overcome this problem, the concept of a 'generic mesh' was introduced.[1] The use of generic meshes for analysing biological geometry has previously been reported.[2,3] A generic mesh can be thought of as a 'simplified symmetrised facial mask' that contains a known number and distribution of points or 'vertices'. The triangles or 'faces' formed by these vertices are indexed or ordered within the file structure. The generic mesh can be used to standardise the number and distribution of vertices for images of the same individual and between individuals. Using the process of 'conformation', the generic facial mesh can be 'wrapped' around any facial image depending on several anchoring landmarks, whilst the remaining points are mathematically fitted or elastically deformed to maintain the surface topography of the original 3D image.

The conformation process on the preoperative and postoperative 3D facial images produces two meshes, which have the same number of vertices and triangles. Each vertex represents a corresponding point on the pre- and post-operative conformed meshes. The accuracy of the conformation process of the generic facial meshes will determine the precision in relating the corresponding facial points for the analysis. A recent study assessing the accuracy of conformation of a generic mesh for the analysis of facial soft tissue changes reported that the method was valid but the accuracy of the conformation was higher towards the middle of the face than towards the peripheral regions.[4] The study was limited to six anatomical facial regions, namely left cheek, right cheek, left upper lip, philtrum, right upper lip and chin regions, and did not investigate the accuracy of the conformation of the facial mesh at peripheral regions including forehead, eyes and gonial angle region. This is essential when using generic meshes to analyse pan-facial changes, especially at peripheral regions, i.e. assessing the changes of the mandibular gonial region following orthognathic surgery or global facial growth.

Aims

This pilot study evaluated the pan-facial accuracy of conformation of a generic mesh.

Materials and methods

Approval was obtained from the Research ethics committee, MVLS, University of Glasgow Ref: 200150025. Six males and four healthy female adult volunteers with no history of facial deformity or previous surgery in the facial region were recruited and consented to participate in the study.

Participant preparation

Prior to 3D image capture, participants were instructed to wear a head cap (figure 1) and then 34 2-mm-diameter self-adhesive, non-reflective black markers (Diamonte, Apparel accessories Ltd, Guangdong, China) were positioned on each subjects' face using an application tool (Pick-it-up vacuum

Figure 1. The six facial movements that were recorded in the study.

tool, Beadsmith, China). The markers (Figure 2 and Table 1) were placed around the eyes, nose, mouth and cheeks, in addition to the peripheries of the face including the tragus, gonial angle and chin areas. These were readily identifiable on the captured 3D facial model, which minimised digitisation errors of anatomical landmarks during the initial conformation of the facial surface mesh. Fifteen of the markers

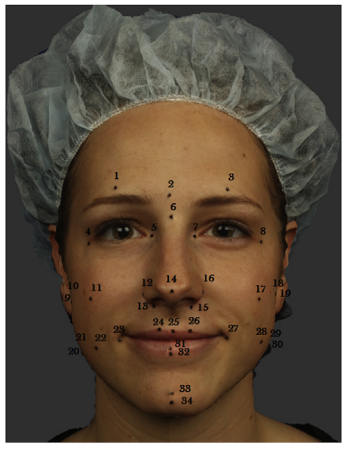

Figure 2. Anatomical position of the facial landmarks.

Table 1
Landmarks definitions, *: mathematically constructed landmarks..

	Abbr.	Landmarks	Definition
1	Eb(R)	Eyebrows-R	The point just above the eyebrows at a vertical line from the pupil
2	Gla	Glabella	The most prominent midline point between eyebrows
3	Eb(L)	Eyebrows-L	The point just above the eyebrows at a vertical line from the pupil
4	Ex(R)	Exocanthion-R	Outer commissure of the eye fissure
5	En(R)	Endocanthion-R	Inner commissure of the eye fissure
6	Na	Nasion	Deepest concavity in the midline at the root of the nose
7	Ex(L)	Exocanthion-L	Outer commissure of the eye fissure
8	En(L)	Endocanthion-L	Inner commissure of the eye fissure
9	Sbtr(R)	Subtragion-R	The most anterior inferior point of the anterior inferior attachment of the ear helix, just above the ear lobe
10	Sbtr(R)1/3*	Subtragion-R (1/3)	One-third the distance from Sbtr(R) to Ala(R)
11	Sbtr(R)2/3*	Subtragion-R (2/3)	Two-third the distance from Sbtr(R) to Ala(R)
12	Ala(R)	Alar curvature-R	Most lateral point on alar contour
13	Ab(R)	Alar base-R	Junction between the right nostril and upper lip
14	Prn	Pronasale	Most protruded point of the apex nasi (tip of the nose)
15	Ab(L)	Alar base-L	Junction between the right nostril and upper lip
16	Ala(L)	Alar curvature-L	Most lateral point on alar contour
17	Sbtr(L)1/3*	Subtragion-L (1/3)	One-third the distance from Sbtr(L) to Ala(L)
18	Sbtr(L)2/3*	Subtragion-L (2/3)	One-third the distance from Sbtr(L) to Ala(L)
19	Sbtr(L)	Subtragion-L	The most anterior inferior point of the anterior inferior attachment of the ear helix, just above the ear lobe
20	Go(R)	Gonion-R	The most lateral point of the cheeks close to mandibular angle.
21	Go(R)1/3*	Gonion-R 1/3	One-third the distance from Go(R) to Ch(R)
22	Go(R)2/3*	Gonion-R 2/3	One-third the distance from Go(R) to Ch(R)
23	Ch(R)	Cheilion-L	Point located at the lateral labial commissure
24	PhL(R)	Philtrum crest-R	The tip of the right philtral ridge at the upper lip vermilion border
25	Ls	Labial superius	Midpoint of the upper vermilion line
26	PhL(L)	Philtrum crest-L	The tip of the right philtral ridge at the upper lip vermilion border
27	Ch(L)	Cheilion-L	Point located at the lateral labial commissure
28	Go(L)2/3*	Gonion-L 1/3	One-third the distance from Go(L) to Ch(L)
29	Go(L)1/3*	Gonion-L 2/3	One-third the distance from Go(L) to Ch(L)
30	Go(L)	Gonion-L	The most lateral point of the cheeks close to mandibular angle.
31	Li+3*	Labial inferius	Midpoint on the lower vermilion line 3 mm higher than Li
32	Li	Labial inferius	Midpoint of the lower vermilion line
33	Pog+3*	Pogonion+3	Midline point 3 mm higher than pogonion
34	Pog	Pogonion	Most prominent midline point of the chin

were used for the conformation process (figure 3), whilst the remaining 19 were used exclusively for the analysis of the accuracy of the method.

For each participant, five facial expressions and the baseline relaxed posture were captured using the Di3D image capture system (Di3D, Dimensional Imaging, Hillington Park, Glasgow, UK). The participants were instructed to slide the mandible forward to resemble a prognathic mandible, slide the mandible to the left to resemble mandibular asymmetry, puff the cheek, purse the lip, and smile to test the accuracy of the conformation process of the generic facial mesh with the various facial expressions (Figure 1).

3D image capture and processing

Each participant was positioned for 3D image capture according to a standardised protocol. A Di3D passive stereophotogrammetry system was used to capture each of the six facial expressions. In total, 60 3D images were captured. The images were individually built to produce a 3D facial model, which was viewed using the Di3D View software (Di3D View, Dimensional Imaging, Hillington Park, Glasgow, UK) and saved in Wavefront (OBJ) format. All the captured images were converted from Wavefront (OBJ) to VRML (WRL) files using the 3DSMax© software (3DSMax Autodesk, Inc., 2002 Microsoft Corporation). The texture information, dimensional units and the orientation of the image were maintained during the conversion process.

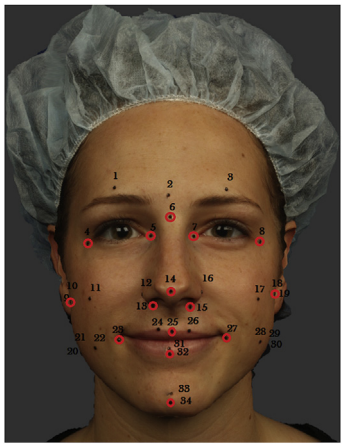

Figure 3. The fifteen landmarks used for the initial conformation phase.

Conformation process

For each individual, the facial mesh in the rest position was used as the generic mesh. The conformation process (elastic deformation) was then performed to warp the generic mesh (at rest) onto each of the other five facial expression images. The in-house developed conformation software provided a dual display panel, one for the generic mesh image (at rest image) and the second for one of the five facial expressions. The conformation process was conducted in two steps: *initial semi-automatic non-linear warping* followed by a *final fully automated conformation*. To start the process, 15 landmarks (Figure 3) were digitised on both the generic mesh and their corresponding locations on the 3D images of each of the five facial expressions. Each landmark was digitised at the centre of the 2 mm prefixed markers on the face. From the 15 selected corresponding landmarks, the generic mesh of the 3D facial image at rest was warped to each of the facial images (the target image) of the five expressions. To achieve the final conformation process, the generic mesh was elastically deformed (warped) over the target image to resemble the shape of the mesh of the facial expression. The conformed images, of the five facial expressions, were exported as a VRML (WRL) file and saved for further analyses. The procedure was repeated for the 10 participants and produced 50 conformed meshes in total.

Errors of the method

To assess the errors of the method, 10 randomly selected images, one from each case, were landmarked twice, with a 2-week interval, by the same operator (AAM). Both the absolute directional (x, y, and z) distances and the Euclidean distances between the repeated digitisation of the same landmark were calculated.

Analysis

Following the conformation of the generic mesh at the rest position and to each of the facial expressions, the 19 landmarks that were not used during conformation were used for the analysis of the accuracy of the process. The mean Euclidian distance between the actual position of these landmarks on the non-conformed expression mesh and the same landmarks on the conformed generic mesh indicated the accuracy of the conformation process. This was performed for each facial expression of the 10 volunteers. The closer the mean distance to zero, the more accurate the conformation process is.

In addition, the classical *inter-surface distance* (mean absolute distances) was measured between the non-conformed surface mesh and the conformed generic mesh based on the 90th percentile of the vertices of these meshes. A distance colour map was generated for the visual illustration of the

conformation process. The data produced from each set of measurements were saved in Microsoft Excel (Microsoft®, Redmond, CA) file for further analysis.

Results

Error of the method

For errors of the landmarking, the mean Euclidean distance and standard deviation for each of the 34 landmarks are shown in Table 2. The overall mean error for all the landmarks was 0.25 ± 0.10 mm. Landmarks 6 (nasion) and 8 (endocanthion left) had the lowest errors, 0.11 ± 0.05 mm and 0.11 ± 0.10 mm, respectively, whilst landmark 30 (gonion left) had the largest error, 0.53 ± 0.62 mm.

Accuracy of conformation

Euclidian distances between the 19 landmarks on the non-conformed expression mesh and the same landmarks on the conformed generic mesh provided a measure of the accuracy of the

Table 2
Mean Euclidean distance and standard deviation for landmarking errors for each of the 34 landmarks.

Landmark number	Abbreviation	Landmarks	Mean (mm)	SD (mm)	95% Confidence interval	
					Lower	Upper
1	Eb(R)	Eyebrows-Right	0.20	0.15	0.08	0.3
2	Gla	Glabella	0.17	0.10	0.09	0.24
3	Eb(L)	Eyebrows-Left	0.15	0.05	0.11	0.19
4	Ex(R)	Exocanthion-Right	0.14	0.10	0.06	0.21
5	En(R)	Endocanthion-Right	0.13	0.10	0.05	0.2
6	Na	Nasion	0.11	0.05	0.05	0.14
7	Ex(L)	Exocanthion-Left	0.18	0.12	0.09	0.27
8	En(L)	Endocanthion-Left	0.11	0.10	0.03	0.18
9	Sbtr(R)	Subtragion-Right	0.18	0.12	0.07	0.24
10	Sbtr(R)1/3[a]	Subtragion-Right (1/3)	0.16	0.09	0.09	0.23
11	Sbtr(R)2/3[a]	Subtragion-Right (2/3)	0.22	0.12	0.13	0.30
12	Ala(R)	Alar curvature-Right	0.21	0.17	0.06	0.32
13	Ab(R)	Alar base-Right	0.22	0.16	0.13	0.22
14	Prn	Pronasale	0.18	0.09	0.12	0.24
15	Ab(L)	Alar base-Left	0.22	0.09	0.13	0.27
16	Ala(L)	Alar curvature-Left	0.19	0.12	0.08	0.27
17	Sbtr(L)1/3[a]	Subtragion-Left (1/3)	0.16	0.11	0.07	0.24
18	Sbtr(L)2/3[a]	Subtragion-Left (2/3)	0.30	0.27	0.09	0.49
19	Sbtr(L)	Subtragion-Left	0.34	0.23	0.13	0.47
20	Go(R)	Gonion-Right	0.17	0.07	0.09	0.21
21	Go(R)1/3[a]	Gonion-Right 1/3	0.16	0.08	0.10	0.20
22	Go(R)2/3[a]	Gonion-Right 2/3	0.21	0.11	0.13	0.29
23	Ch(R)	Cheilion-Left	0.15	0.08	0.09	0.21
24	PhL(R)	Philtrum crest-Right	0.22	0.11	0.12	0.30
25	Ls	Labial superius	0.31	0.28	0.11	0.50
26	PhL(L)	Philtrum crest-Left	0.16	0.10	0.08	0.24
27	Ch(L)	Cheilion-Left	0.19	0.09	0.12	0.25
28	Go(L)2/3[a]	Gonion-Left 1/3	0.25	0.17	0.11	0.37
29	Go(L)1/3[a]	Gonion-Left 2/3	0.27	0.07	0.17	0.31
30	Go(L)	Gonion-Left	0.53	0.62	0.07	0.97
31	Li+3[a]	Labial inferius	0.36	0.20	0.21	0.50
32	Li	Labial inferius	0.43	0.36	0.15	0.68
33	Pog+3[a]	Pogonion+3	0.43	0.29	0.21	0.63
34	Pog	Pogonion	0.33	0.10	0.23	0.4
Overall mean and standard deviation of landmarking errors			**0.25**	**0.10**		

[a] Constructed landmarks.

Table 3
Mean absolute distance between meshes (mm).

Cases	Lateral mandible shift		Cheek puff		Forward mandible shift		Smile		Lip purse	
	Absolute mean	SD	Absolute mean	SD	Absolute mean	SD	Absolute mean	SD	Absolute mean	SD
1	0.04	0.08	0.04	0.07	0.04	0.06	0.04	0.07	0.04	0.09
2	0.00	0.03	0.00	0.07	0.00	0.02	0.00	0.02	0.00	0.03
3	0.05	0.1	0.06	0.1	0.06	0.1	0.06	0.1	0.06	0.11
4	0.00	0.03	0.00	0.01	0.00	0.01	0.00	0.01	0.00	0.02
5	0.02	0.03	0.02	0.01	0.02	0.03	0.02	0.06	0.02	0.04
6	0.02	0.02	0.02	0.01	0.02	0.01	0.02	0.01	0.02	0.01
7	0.02	0.04	0.02	0.03	0.02	0.03	0.02	0.03	0.02	0.03
8	0.00	0.01	0.00	0.02	0.00	0.01	0.00	0.01	0.00	0.03
9	0.02	0.17	0.02	0.12	0.00	0.05	0.00	0.02	0.00	0.05
10	0.00	0.02	0.00	0.01	0.00	0.01	0.00	0.01	0.00	0.01

conformation process (Table 3). The minimum mean Euclidean distance between the corresponding landmarks was at philtrum crest right, 0.73 ± 0.24 mm (95% CI 0.62–0.99 mm), whilst the maximum distance was at gonion right, 1.74 ± 0.64 mm (95% CI 1.33–2.37 mm). The mean Euclidean distance error of the conformation process was 1.13 ± 0.26 mm.

The effect of each facial expression on the accuracy of the conformation is shown in Table 4. On the basis of the accuracy of the conformation process, the five facial expressions were ranked in ascending order, starting with the lateral mandible shift, lip purse, forward mandible shift, cheek puff and smile. The lowest errors (1.06 ± 0.33 mm) of the conformation process of the facial mesh were associated with the lateral mandible shift expression, and the maximum inaccuracy of the conformation process was related to maximum smile, which was 1.46 ± 0.51 mm (Table 5).

Table 3 shows the accuracy of the conformation process based on the mean absolute distances between the conformed and the original meshes. The largest distance was 0.06 mm, which was observed in subject 3 across all facial expressions.

Table 4
Mean Euclidean distances (mm) of the 19 corresponding landmarks between the conformed and original mesh for all facial expressions.

Landmark number	Abbreviations	Landmarks names	Mean (mm)	SD (mm)	95% Confidence interval	
					Lower	Upper
1	Eb(R)	Eyebrows-Right	1.27	0.34		
2	Gla	Glabella	0.77	0.36	1.11	1.65
3	Eb(L)	Eyebrows-Left	1.19	0.31	0.56	1.10
10	Sbtr(R)1/3[a]	Subtragion-Right (1/3)	1.20	0.45	1.06	1.53
11	Sbtr(R)2/3[a]	Subtragion-Right (2/3)	1.21	0.39	0.93	1.68
12	Ala(R)	Alar curvature-Right	1.17	0.46	1.02	1.6
16	Ala(L)	Alar curvature-Left	1.07	0.32	0.87	1.55
17	Sbtr(L)1/3[a]	Subtragion-Left (1/3)	1.18	0.40	0.89	1.38
18	Sbtr(L)2/3[a]	Subtragion-Left (2/3)	1.14	0.34	0.96	1.59
20	Go(R)	Gonion-Right	1.74	0.64	0.97	1.50
21	Go(R)1/3[a]	Gonion-Right 1/3	1.37	0.55	1.33	2.37
22	Go(R)2/3[a]	Gonion-Right 2/3	0.76	0.43	1.10	1.88
24	PhL(R)	Philtrum crest-Right	0.81	0.22	0.49	1.17
26	PhL(L)	Philtrum crest-Left	0.73	0.24	0.72	1.07
28	Go(L)2/3[a]	Gonion-Left 1/3	1.05	0.64	0.62	0.99
29	Go(L)1/3[a]	Gonion-Left 2/3	1.41	0.43	0.63	1.56
30	Go(L)	Gonion-Left	1.44	0.40	1.22	1.85
32	Li	Labial inferius	0.96	0.34	1.24	1.83
34	Pog	Pogonion	0.97	0.83	0.77	1.24
Overall mean distance			**1.13**	**0.26**	**0.43**	**1.65**

[a] Constructed landmarks.

Table 5
Mean Euclidean distance between the corresponding landmarks for each facial expression (mm).

Landmark number	Landmarks		Lateral mandible shift	Cheek puff	Forward mandible shift	Smile	Lip purse	Mean (mm)	SD (mm)
			Mean	Mean	Mean	Mean	Mean		
1	Eb(R)	Eyebrows-R	1.87	1.1	1.25	1.62	1.07	1.38	0.35
2	Gla	Glabella	1.08	0.58	1.01	0.97	0.50	0.83	0.27
3	Eb(L)	Eyebrows-L	1.23	1.23	1.43	1.50	1.08	1.29	0.17
10	SbtrR 1/3	Subtragion-R (1/3)	1.09	1.65	0.82	1.85	1.11	1.3	0.43
11	SbtrR 2/3	Subtragion-R (2/3)	1.08	1.95	0.78	1.63	1.10	1.31	0.47
12	Ala(R)	Alar curvature-R	0.96	1.76	0.98	1.02	1.35	1.21	0.35
16	Ala(L)	Alar curvature-L	0.99	1.67	0.66	0.93	1.44	1.14	0.41
17	Sbtr L 1/3	Subtragion-L (1/3)	0.83	2.03	0.88	1.60	1.04	1.28	0.52
18	Sbtr L 2/3	Subtragion-L (2/3)	0.94	1.62	0.80	1.81	1.01	1.24	0.45
20	Go(R)	Gonion-R	1.40	1.58	2.49	2.51	1.27	1.85	0.60
21	Go(R) 1/3	Gonion-R 1/3	1.31	1.76	0.97	1.80	1.62	1.49	0.35
22	Go(R) 2/3	Gonion-R 2/3	0.70	0.84	0.77	0.97	0.87	0.83	0.10
24	PhL(R)	Philtrum crest-R	0.69	1.03	0.72	1.16	0.87	0.89	0.20
26	PhL(L)	Philtrum crest-L	0.53	0.90	0.66	1.11	0.83	0.81	0.23
28	Go(L)2/3	Gonion-L 1/3	0.78	1.25	1.07	1.30	1.08	1.10	0.20
29	Go(L) 1/3	Gonion-L 2/3	0.99	1.65	1.38	2.11	1.53	1.53	0.41
30	Go(L)	Gonion-L	1.51	1.41	1.35	2.15	1.23	1.53	0.36
32	Li	Labial inferius	1.39	0.68	1.16	0.61	1.19	1.01	0.34
34	Pog	Pogonion	0.74	0.76	1.89	0.99	0.82	1.04	0.48
Overall mean			1.06	1.34	1.11	1.46	1.11	**1.21**	**0.28**
SD			0.33	0.45	0.46	0.51	0.27		

Discussion

Dense correspondence analysis has been reported as an efficient method of analysing morphological changes, which may explain its broad applications in the medical field.[3] However, despite its accuracy and comprehensiveness in soft tissue analyses, this approach is largely dependent on '3D model elastic deformation', in which the generic facial mesh is elastically deformed to reproduce the individual's facial features. The initial step of the conformation process involved the translation of the corresponding landmarks to match their positions on the target image, followed by elastic deformation to minimise the bending energy (thin plate spline). This process included both shape and positional changes. In this study, the six facial postures were captured in the same session, which provided a relatively close starting point for the conformation process. Despite the fact that only 10 volunteers participated in this study, each of the facial postures was considered an individual case, therefore; the total number of images involved in the study was 50. A total of 15 landmarks were used to execute the conformation procedure. To eliminate bias, these landmarks were excluded from the analysis of the accuracy of the conformation procedure.

The accuracy of the conformation process has been previously reported.[5,6] In these studies, the accuracy was determined by measuring the inter-surface distance between the conformed mesh and the target models. The disadvantage of this approach is that the magnitude of error is measured as the distance between the closest points on the two surface meshes, namely the target model and the conformed mesh, and not the distances between the actual anatomical corresponding points. Measuring the closest distance between two meshes would not necessarily detect the potential sliding of the surface meshes over one another during the conformation process, which would provide a misleadingly low estimate of the conformation errors. However, the assessment of the accuracy of the conformation process based on specific landmarks also carries the risk of overestimating the accuracy of the conformation process as only a single point on the mesh is analysed, whilst the remainder of the mesh is not assessed.

The Euclidian distance between the actual landmarks on the non-conformed mesh and the landmarks on the conformed generic mesh, for the same facial expression, was used as a measure of

accuracy of the conformation process. Although this was not a comprehensive surface-based analysis, its robustness was maximised by carefully selecting the landmarks to represent various anatomical regions of the face, which was believed to be clinically relevant.

The analysis was repeated using the classical inter-surface distances based on the 90th percentile of the vertices of the two meshes and measuring the mean distances between the conformed mesh and original mesh for all facial expressions. This measure takes into account the direction of error and produces positive and negative values, which depend on the spatial location of the meshes relative to each other. Despite the fact that these measurements are descriptive to the magnitude and the direction of the conformation errors, the mean value of these measurements are underestimated as the positive and negative measurements would cancel each other. Moreover, the Euclidean distances measure the shortest distances between corresponding points on the two surface meshes, irrespective of the directionality of the mismatch between the two surface meshes; therefore, the arithmetic average value of these distances is more meaningful. As expected, the error based on the mean absolute distances is much smaller than those based on the Euclidian distances.

Two main factors may contribute to the errors in the conformation process. First, and the most important, is the accuracy and reproducibility of the digitisation of the landmarks, which are used in the initial conformation stage. This was minimised in the present study through pre-landmarking. The second source of errors depends on the deficiency in the algorithm of the conformation process.[5]

To reduce the effect of landmarking errors, which affects the reliability of the conformation process, 2-mm-diameter round markers were pre-placed on 34 anatomical points on each participant's face. The use of pre-landmark placement significantly reduced the landmarking error and allowed the conformation process to be analysed comprehensively by eliminating this potential source of error.[7] The round shape of the landmark facilitated accurate landmark digitisation, with a mean error of 0.23 ± 0.11 mm.

The presented innovative approach provides a useful tool for 3D analysis of the face; it provides comprehensive evaluation of the morphological characteristics, which is superior to assessment at a limited set of individual landmarks. The method allows the analysis of facial asymmetries and both the typical and abnormal growth patterns. It can be applied for the evaluation of a sequence of 3D facial images (4D) for the analysis of the dynamics of facial expressions. We expect the method to be fully integrated as a clinical tool with various surgical specialities to improve the quality of diagnosis and prediction planning of corrective facial surgeries. The limitation associated with the visualisation of 3D facial model on a flat screen can be solved with the production of 3D objects using the innovation of 3D printing and rapid prototyping.[8]

The results of this study confirmed that landmarks around the lips and nose (in the midline) were associated with lower level of conformation errors compared to those around the borders of the image such as cheeks and gonial angle regions, which is in agreement with previous studies.[4] This might be due to the lack of details of surface topography, upon which the elastic deformation relied, in conjunction with the absence of well-defined landmarks around the lower border and gonial angle region. This should be taken onto account when using this technique in facial analysis following orthognathic surgery. The changes around the lower border and gonial angle should be viewed with caution as they showed a higher level of inaccuracy as indicated by the upper 95% confidence limit of around 2.0 mm.

Conclusions

The conformation procedure has a 1–2 mm level of accuracy, with a higher level of accuracy in the midline and less accuracy peripherally. This technique has broad clinical applications including facial analysis of the impact of orthognathic surgery in changing facial morphology and monitoring of facial growth.

Funding and conflict of interest

None.

References

1. Khambay B, Ullah R. Current methods of assessing the accuracy of three-dimensional soft tissue facial predictions: Technical and clinical considerations. *Int J Oral Maxillofac Surg*. 2015;44(1):132–138.
2. Claes P, Walters M, Clement J. Improved facial outcome assessment using a 3D anthropometric mask. *Int J Oral Maxillofac Surg*. 2012;41(3):324–330.
3. Claes P, Walters M, Vandermeulen D, Clement JG. Spatially-dense 3D facial asymmetry assessment in both typical and disordered growth. *J Anat*. 2011;219(4):444–455.
4. Cheung MY, Almukhtar A, Keeling A, et al. The accuracy of conformation of a generic surface mesh for the analysis of facial soft tissue changes. *PLoS One*. 2016;11(4), e0152381.
5. Mao Zhili, Ju Xiangyang, Paul Siebert J, Paul Cockshott W, Ashraf Ayoub. Constructing dense correspondences for the analysis of 3D facial morphology. *Pat Recog Lett*. 2006;27:597–608.
6. Chabanas M, Luboz V, Payan Y. Patient specific finite element model of the face soft tissues for computer-assisted maxillofacial surgery. *Med Image Anal*. 2003;7:131–151.
7. Aynechi N, Larson BE, Leon-Salazar V, Beiraghi S. Accuracy and precision of a 3D anthropometric facial analysis with and without landmark labeling before image acquisition. *Angle Orthod*. 2011;81(2):245–252.
8. Rengier F, Mehndiratta A, von Tengg-Kobligk H, et al. 3D printing based on imaging data: Review of medical applications. *Int J CARS*. 2010;5:335–341.